AFRL-AFOSR-JP-TR-2019-0042

GeSn Based Near and Mid Infrared Heterostructure Detectors 2

Greg Sun
UNIVERSITY OF MASSACHUSETTS
100 MORRISSEY BLVD RM 80
BOSTON, MA 02125-3300

07/05/2019
Final Report

Air Force Research Laboratory
Air Force Office of Scientific Research
Asian Office of Aerospace Research and Development
Unit 45002, APO AP 96338-5002

REPORT DOCUMENTATION PAGE		*Form Approved* *OMB No. 0704-0188*

The public reporting burden for this collection of information is estimated to average 1 hour per response, including the time for reviewing instructions, searching existing data sources, gathering and maintaining the data needed, and completing and reviewing the collection of information. Send comments regarding this burden estimate or any other aspect of this collection of information, including suggestions for reducing the burden, to Department of Defense, Executive Services, Directorate (0704-0188). Respondents should be aware that notwithstanding any other provision of law, no person shall be subject to any penalty for failing to comply with a collection of information if it does not display a currently valid OMB control number.
PLEASE DO NOT RETURN YOUR FORM TO THE ABOVE ORGANIZATION.

1. REPORT DATE *(DD-MM-YYYY)* 05-07-2019	**2. REPORT TYPE** Final	**3. DATES COVERED** *(From - To)* 20 Sep 2017 to 19 Mar 2019

4. TITLE AND SUBTITLE GeSn Based Near and Mid Infrared Heterostructure Detectors 2	**5a. CONTRACT NUMBER**
	5b. GRANT NUMBER FA2386-17-1-4100
	5c. PROGRAM ELEMENT NUMBER 61102F
6. AUTHOR(S) Greg Sun	**5d. PROJECT NUMBER**
	5e. TASK NUMBER
	5f. WORK UNIT NUMBER

7. PERFORMING ORGANIZATION NAME(S) AND ADDRESS(ES) UNIVERSITY OF MASSACHUSETTS 100 MORRISSEY BLVD RM 80 BOSTON, MA 02125-3300 US	**8. PERFORMING ORGANIZATION REPORT NUMBER**

9. SPONSORING/MONITORING AGENCY NAME(S) AND ADDRESS(ES) AOARD UNIT 45002 APO AP 96338-5002	**10. SPONSOR/MONITOR'S ACRONYM(S)** AFRL/AFOSR IOA
	11. SPONSOR/MONITOR'S REPORT NUMBER(S) AFRL-AFOSR-JP-TR-2019-0042

12. DISTRIBUTION/AVAILABILITY STATEMENT
A DISTRIBUTION UNLIMITED: PB Public Release

13. SUPPLEMENTARY NOTES

14. ABSTRACT
This final report presents results obtained and progress made during September 20th, 2017 to March 19, 2019. This project is a part of the greater effort for the development of Si photonics that broadens the reach of Si material and technology beyond electronics. The focus of the project is the development of photonic devices based on the group-IV alloys, SiGeSn and/or GeSn that can be integrated with the CMOS Si technology. In this project, we have made progress on three fronts. One is on the GeSn quantum structures that can benefit a range of photonic devices. The second is on light emitting diodes whose emission can be in-plane coupled into group-IV waveguides and subsequently be detected by GeSn based waveguide detectors. The third includes the demonstration of GeSn based vertical light emitters and optically pumped lasers. This report highlights the main achievements in these three areas.

15. SUBJECT TERMS
GeSn, Germanium-Tin, infrared, photodetectors

16. SECURITY CLASSIFICATION OF:			**17. LIMITATION OF ABSTRACT**	**18. NUMBER OF PAGES**	**19a. NAME OF RESPONSIBLE PERSON** KNOPP, JEREMY
a. REPORT Unclassified	**b. ABSTRACT** Unclassified	**c. THIS PAGE** Unclassified	SAR		**19b. TELEPHONE NUMBER** *(Include area code)* 315-227-7006

Standard Form 298 (Rev. 8/98)
Prescribed by ANSI Std. Z39.18

Final Report for AOARD Grant FA2386-17-1-4100 (AOARD-17IOA100)

"GeSn Based Near and Mid Infrared Heterostructure Detectors"

March 20, 2019

Principal Investigator:
Greg Sun
Engineering Department
The University of Massachusetts at Boston
Boston, MA 02125, USA
greg.sun@umb.edu
Tel: 617-287-6432
Fax: 617-287-6053

Period of Performance: September 20th, 2017 to March 19, 2019

Abstract

This final report presents results obtained and progress made during September 20th, 2017 to March 19, 2019. This project is a part of the greater effort for the development of Si photonics that broadens the reach of Si material and technology beyond electronics. The focus of the project is the development of photonic devices based on the group-IV alloys, SiGeSn and/or GeSn that can be integrated with the CMOS Si technology. In this project, we have made progress on three fronts. One is on the GeSn quantum structures that can benefit a range of photonic devices. The second is on light emitting diodes whose emission can be in-plane coupled into group-IV waveguides and subsequently be detected by GeSn based waveguide detectors. The third includes the demonstration of GeSn based vertical light emitters and optically pumped lasers. This report highlights the main achievements in these three areas.

1) GeSn-based quantum well structures and type-I carrier confinement

The GeSn-based quantum wells (QWs) have been the focus of this study for the achievement of direct bandgap QWs with type-I band alignment that improves carrier confinement [1, 2]. Such QWs are particularly important for developing efficient light emitting devices such as LEDs and lasers. In this work, we conducted the systematic study of light emission from the $Ge_{0.91}Sn_{0.09}/Ge_{0.85}Sn_{0.15}/Ge_{0.91}Sn_{0.09}$ double QW structure. Two double QW samples, with the thicknesses of $Ge_{0.85}Sn_{0.15}$ well of 6 and 19 nm, were investigated as shown in Fig. 1, along with their HRXRD 2θ-ω scans and SIMS plots.
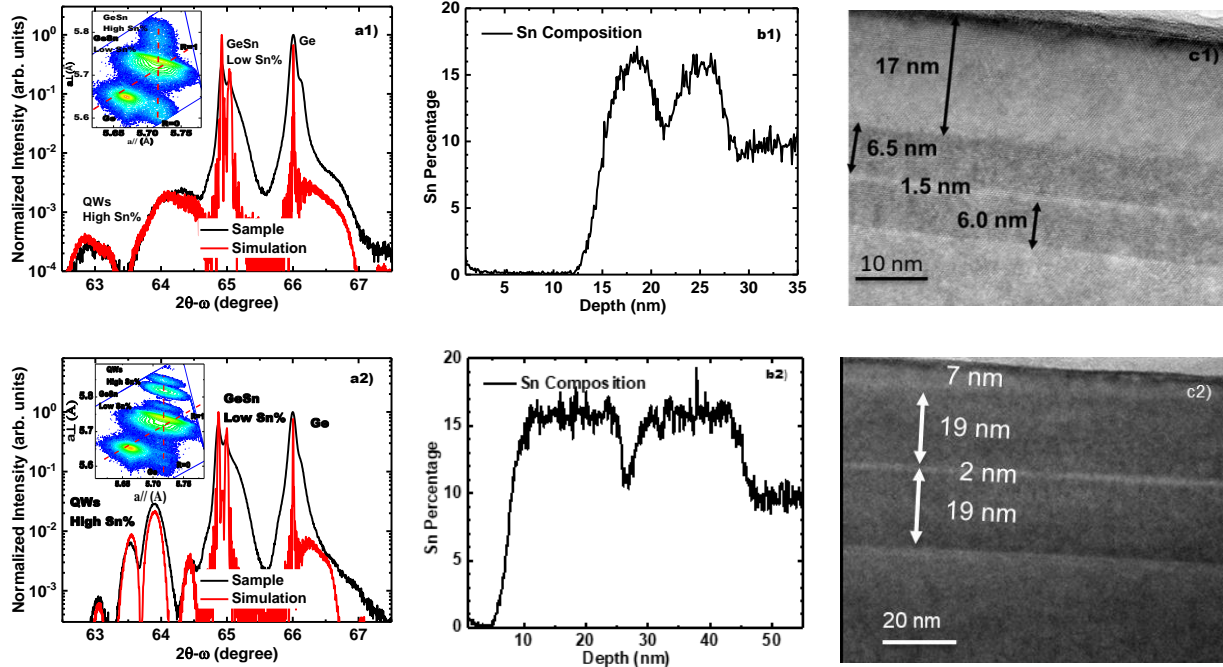
1

Figure 1. (a1) (a2) HRXRD 2θ-ω scan of samples A and B. The black and red curves are measured data and simulation results, respectively. Inset: The RSM contour plot; (b1) (b2) SIMS of samples A and B showing the Sn composition in each layer; (c1) (c2) TEM images of samples A and B.

Band structure calculations revealed that both samples feature type-I band alignment as shown in Fig. 2. By increasing the Sn composition in GeSn barrier and quantum well, the QW layer featured increased energy separation between the indirect and direct bandgaps towards a better direct gap semiconductor. Moreover, the thicker well sample exhibited improved carrier confinement compared to the thinner well sample due to lowered first quantized energy level in the Γ valley.
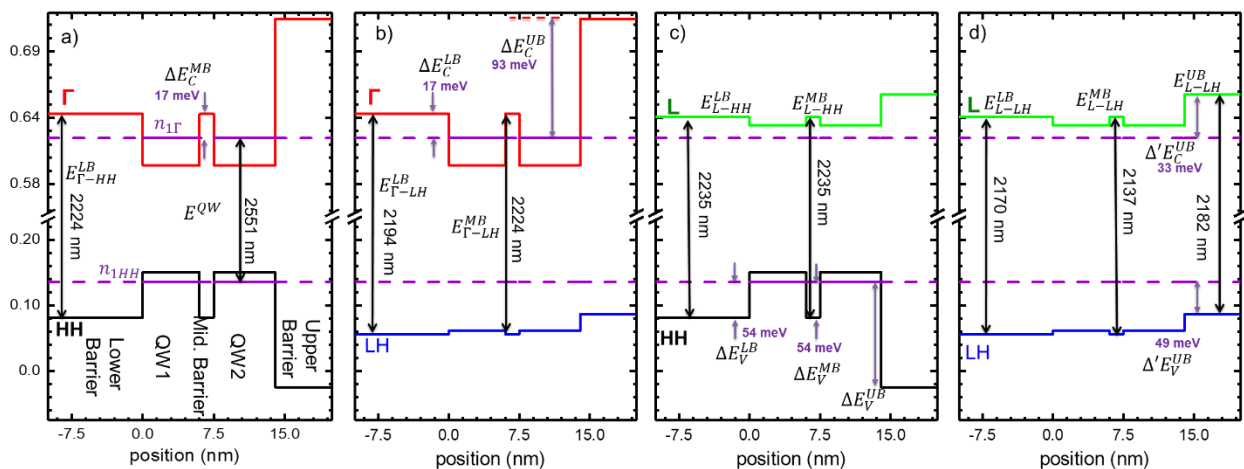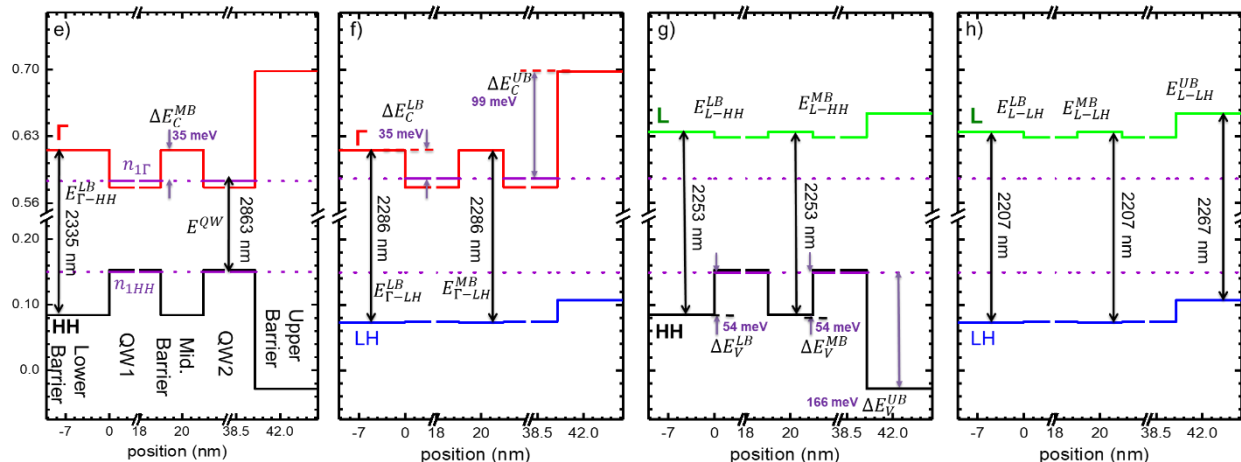
Figure 2. Top: for sample A. Band diagram calculated based on measured material data, showing the carrier confinement and the possible band-to-band optical transitions between (a) Γ-HH; (b) Γ-LH; (c) L-HH; and (d) L-LH. (Unit: meV). Bottom: for sample B. (e)-(h) The similar band diagram and optical transition calculations.

At 300 K, the QW emission peaks at 2560 nm and 2800 nm for samples A and B were observed, respectively. The peak intensity increased dramatically as temperature decreased to 10 K, indicating a typical direct bandgap behavior. The transitions from Ge and GeSn barriers were also obtained and the peaks are partially overlapped due to small energy separation. Comparing samples B to A, the higher Sn composition in well and increased well layer thickness lead to the bandgap more directness and significantly enhanced carrier confinement of sample B. Particularly at lower temperature, the sufficient carrier confinement of sample B results in hundreds times integrated PL intensity increase under CW pump lasers, and the QW emissions dominating the PL under both CW and pulse pump lasers.

2) Room-temperature GeSn light-emitting diode for in-plane coupling to group-IV waveguides

This work is a study on a Si-based GeSn p-i-n homojunction light-emitting diode (LED) designed as an on-chip light source for integrated-photonic applications such as chem-bio sensing and short-reach optical communications [3]. The room-temperature LED emits primarily in-plane, unlike the prior-art Ge/GeSn/Ge heterojunction PIN diodes that emit mainly vertically into free space. The schematic of the LED structure is shown in Fig. 3, which is deliberately constructed to have the following features: (1) ease of manufacture in a foundry via a simple epitaxial structure, (2) ease of end-fire coupling into on-chip transparent Ge or Si waveguides in close proximity, (3) emission in the new 2-µm communications band where new low-loss fibers operate, (4) ion implanted P and N doping, (5) ease of making source arrays, (6) monolithic construction for the "all-group-IV" photonics scenario, and (7) compatibility with photonic and optoelectronic circuits.
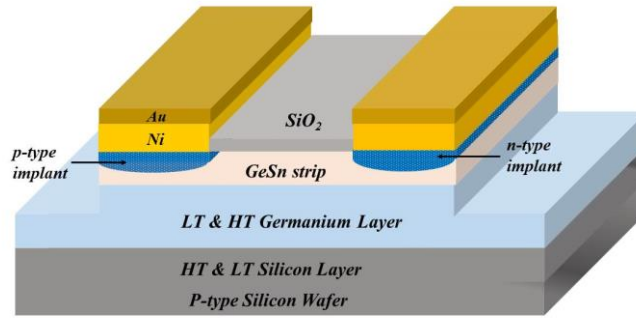
3

Figure 3. Schematic of the GeSn-based mesa diode that couples into an in-plane waveguide.

Because the index of refraction of the intrinsic GeSn region is higher than that of its surroundings, light is partially confined in that GeSn "core", giving channel waveguiding that causes directionality of infrared emission along the long axis of the mesa. We estimate that 30% of the total 4π steradian emission is emitted from each of two end facets, and that 40% of the total is emitted into the substrate-and-superstrate regions. The end-fire emission from a facet is ideal for direct butt-coupling to an adjacent inline transparent Si or Ge channel waveguide. The present mesa is a low-Q Fabry Perot cavity with uncoated mirrors.
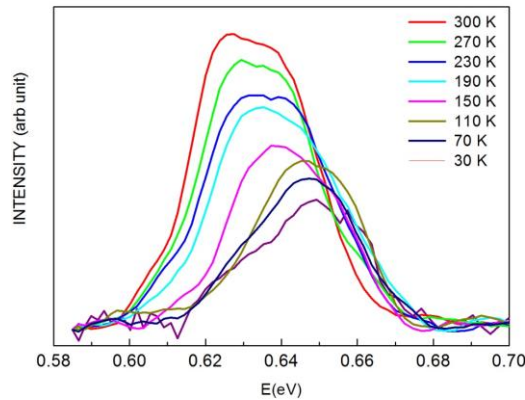

Figure 4. Temperature-dependent electroluminescence spectrum of the sample.

The EL spectra under injection, with a current density of 0.362 A/cm^2 are plotted in Fig.4 across the spectral window of 0.58 to 0.70 eV. At room temperature, a broad feature is observed with a peak energy at 0.63 eV (1.968 μm). This is below the indirect bandgap of bulk Ge of 0.66 eV; therefore, this observation is attributed to signals originating from the GeSn. As mentioned, the signal is associated with an indirect optical transition. With a reduction in the temperature, the peak position of the spectrum progressively shifts to a higher energy, reflecting the characteristic

4

of a band-to-band optical transition associated with the increase of the energy bandgap of GeSn, consistent with previous reports.

This study shows that ion implantation is a practical alternative to the conventional method of incorporating dopants during epitaxy. The ion technique has several advantages; the fabrication process is CMOS compatible, the doping level in the area can be increased simply by changing the dose level (or the energy of the ion beam), and it is not limited by the *solid solubility* of Sb in Ge (or B in Ge) which limits conventional doping. The dopant level is important for the case of a GeSn photodiode because the diode's responsivity increases as the dopant level at the electrodes increases. Most importantly, this implies that both emitters and detectors can be fabricated within the same GeSn layer, providing a path for "complete" integration of group IV optoelectronics.

3) GeSn based vertical light emitters and optically pumped lasers

We have demonstrated the first electrically-injected GeSn vertical-cavity surface emitter (VCSE) grown on SOI substrates [4]. We introduce a vertical cavity with the GeSn active layer to enhance the light emitting efficiency. Figure 1(a) illustrates a schematic diagram of the p-i-n Ge/GeSn/Ge double barrier heterostrucrure (DHB) VCSE grown on an SOI substrate via a virtual substrate (VS). The p-i-n structure features a GeSn active layer with reduced energy difference between the direct and indirect conduction band edges, compared to pure Ge for enhancing direct transitions. In addition, the buried oxide (BOX) layer and the deposited SiO_2 layer serve as the top and bottom reflectors, respectively, because of their much lower refractive index (~1.45) compared to the GeSn p-i-n structure (~4.2), creating a vertical Fabry-Perot-like cavity for the GeSn active layer to enhance the light emission. Figure 1(b) shows a schematic band diagram of the GeSn active layer. The introduction of Sn into the active layer lower the energy difference between the direct and indirect conduction band edges for enhancing light emission accomplished by direct transitions. In addition, growing GeSn layers on Ge VS induces an important compressive strain which lifts the degeneracy of the heavy-hole (HH) and light-hole (LH) bands. As the result, the top valence band is HH band and the lowest direct transition is from the Γ-conduction band to HH band (cΓ→HH) which dominates the light emission process under current injection.

Figure 6(a) shows the measured room-temperature EL spectra under different continuous-wave (CW) injected forward currents. It is seen that the emission spectra exhibit clear oscillation features with a free spectral range of ∼110 nm, providing evidences for the longitudinal resonant cavity modes in the GeSn vertical cavity. Among these emission peaks, two distinguishable strongest emission peaks located at λ_1∼1767 nm and λ_2∼1886 nm are found, labeled as peaks 1 and 2, respectively. Measured EL spectrum and the mode envelops at I=250 mA are shown in Fig. 6(b). To extract the GeSn direct bandgap energy, Figure 6(c) shows the envelopes of the EL emission spectra under different injected currents, where the envelope maximum (λ_p) is indicated by gray dots, which represents the lowest direct bandgap (cΓ→HH) of the GeSn active layer. The envelope maximum as a function of the injected current is depicted in Fig. 6(d). For low injected current <100 mA, the envelope maximum is located at 1780~nm, corresponding to the cΓ→HH direct

5

transition energy of 0.696 eV. As a result, peak 1 is the cavity mode near the band edge (<1781 nm) that dominates the emission process. As the injected current increases, a redshift of the envelope is clearly observed and it becomes more apparent at higher injected currents, indicating important bandgap narrowing (BGN). Although higher injected current (carriers) will decrease the refractive index in the cavity that will result in blue shift of emission spectra, the observed BGN here is mainly attributed to the increased junction temperature resulting from the Joule heating effect. Because of the BGN effect, peak 2 becomes the cavity mode near the band edge at higher injected currents and then dominates the radiative processes. Figure 6(e) presents the integrated EL intensity (L) as a function of the injected current at room temperature. The L-I curve shows that the integrated EL intensity increases rapidly with increasing injected current. The L-I curve can be characterized using $L = AI^m$, where A is a constant and the m factor is related to the light emission efficiency. The extracted m-factor at different injected currents is displayed in Fig. 6(f). The m factor increases rapidly from 1.88 at I=60 mA to 4.43 at I=240 mA, highlighting higher EL efficiency at higher currents. This EL enhancement is attributed to the increased junction temperature caused by the Joule heating effect that not only reduces $\Delta E_{\Gamma L}$ (discussed later), but also thermally excites more electrons from the L-conduction band to the Γ-conduction band, enhancing the direct-gap transitions.
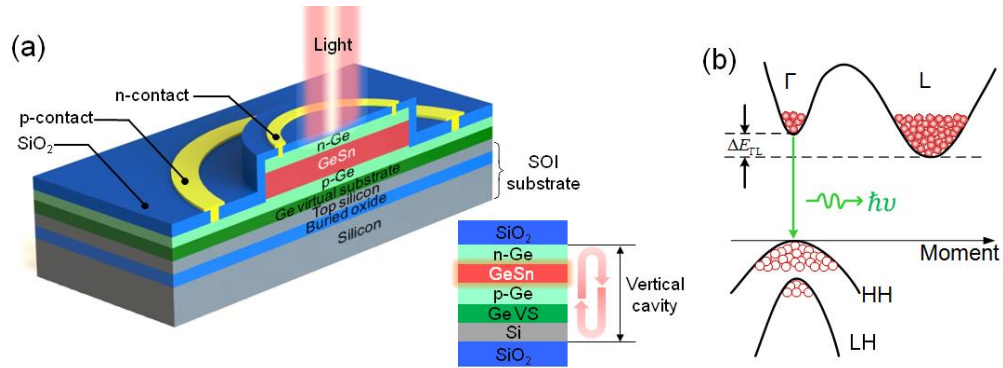

Figure 5. (a) Schematic of our GeSn p-i-n hetero-diode vertical-cavity surface emitter grown on silicon-on-insulator substrates. The buried oxide serves as the bottom reflector and the deposited SiO2 layer serves as the top reflector, creating a vertical cavity for enhancing the light emitting efficient of the GeSn active layer. (b) Schematic band diagram of the $Ge_{0.969}Sn_{0.031}$ active layer.

The room-temperature EL experiment demonstrates clear resonant cavity modes which considerably enhance the light emitting efficiency. Analysis of optical gain suggests important absorption bleaching at room temperature in the GeSn cavity, towards achieving net optical gain in the devices. In addition, temperature effects on optical gain and loss are discussed for achieving net optical gain in the GeSn cavity. These results pave the way towards electrically-injected GeSn lasers operating at room temperature or higher for practical EPIC applications.
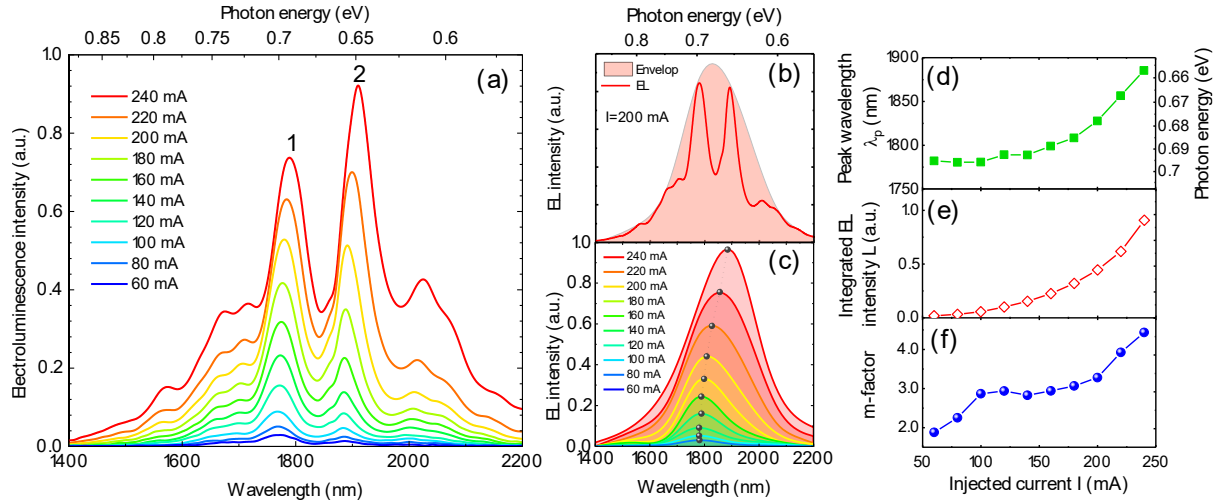
6

Figure 6. (a) Room temperature EL spectra of the GeSn VCSE measured under different injected currents. (b) Measured EL spectrum and the mode envelops at I=250 mA. (c) Mode envelopes at different injected currents. The peak wavelength of the mode envelope is indicated by gray dots. (d) Peak wavelength of the mode envelope, (e) integrated EL intensity, and (f) m factor extracted from the EL spectra as a function of injected current density.

The TEM image showed a two-layer GeSn film, where a defect-free top GeSn layer was obtained. A wet chemical etching process was developed to fabricate the ridge waveguide with smooth sidewalls achieved. Temperature-dependent characteristics of laser-output versus pumping-laser-input were investigated. The unambiguous lasing operation was observed up to 110 K. The laser mode was analyzed via high-resolution PL spectra, which revealed the multimode operation of the laser. The lasing threshold and operation wavelength were measured as 68 kW/cm^2 and 2476 nm at 10 K, respectively. Based on the temperature-dependent threshold, a characteristic temperature of 65 K was extracted. According to the band structure calculation and the lasing mode profile analysis, the optimizing solution for laser structure was proposed, which could reduce the lasing threshold and increase the operating temperature. The capability of producing the GeSn laser in a "manufacture ready" process (industry reactor, low cost precursor, and single run epitaxy process) indicates the great potential of GeSn to be easily adopted by future foundry for integrated photonics applications when the material is mature.

We have also investigated optically pumped GeSn lasers with ridge and planar waveguide structures were investigated [5-7]. The GeSn samples were grown using a multiple-step Sn-enhanced growth recipe via industry standard CVD reactor with low-cost SnCl$_4$ and GeH$_4$ precursors. The maximum Sn composition of 20% was obtained. A wet chemical etching process was developed to fabricate the ridge waveguide with smooth sidewalls achieved. Temperature-dependent characteristics of laser-output versus pumping-laser-input were investigated. The unambiguous lasing operation was observed up to 110 K. The laser mode was analyzed via high-resolution PL spectra, which revealed the multimode operation of the laser. The lasing threshold and operation wavelength were measured as 68 kW/cm^2 and 2476 nm at 10 K, respectively. Based

7

on the temperature-dependent threshold, a characteristic temperature of 65 K was extracted. According to the band structure calculation and the lasing mode profile analysis, the optimizing solution for laser structure was proposed, which could reduce the lasing threshold and increase the operating temperature. Our latest result shows that maximum operating temperature of 270 K was achieved. At 280 K, stimulated emission spectrum was observed with intensive pumping power density. Our systemic study of the four optically pumped laser devices with various ridge width reveals that the reduced side-wall surface recombination and better heat dissipation are key factors to achieve near room temperature operation. We predict that room temperature GeSn lasers can be demonstrated by: i) surface passivation (adding Ge cap layer) to further reduce the surface recombination and ii) optimization of the ridge width to strike a balance between the heat dissipation and optical confinement. The demonstration of planar waveguide laser structure in this study points at the great potential of GeSn lasers being advanced towards high-performance Si-based monolithically integrated mid-infrared coherent light sources.

References (also our publications during the performance period)

1. P. Grant, J. Margetis, W. Du, Y. Zhou, W. Dou, G. Abernathy, A. Kuchuk, B. Li, J. Tolle, J. Liu, G. Sun, R. Soref, M. Mortazavi, S.-Q. Yu, "Study of direct bandgap type-I GeSn/GeSn double quantum well with improved carrier confinement," *Nanotechnology* **29**, 465201 (2018)
2. P. Grant, J. Margetis, Y. Zhou, W. Dou, G. Abernathy, A. Kuchuk, W. Du, B. Li, J. Tolle, J. Liu, G. Sun, R. A. Soref, M. Mortazavi, and S.-Q. Yu, "Direct bandgap type-I GeSn/GeSn quantum well on a GeSn- and Ge-buffered Si substrate," AIP Advances **8**, 025104 (2018)
3. C. Chang, T.-W. Chang, H. Li, H.-H. Cheng, R. A. Soref, G. Sun, and J. R. Hendrickson, "Room-temperature 2-μm GeSn P-I-N homojunction light-emitting diode for in-plane coupling to group-IV waveguides," Applied Physics Letters **111**, 141105 (2017)
4. G.-E. Chang, B.-J. Huang, Y.-D. Hsieh, R. Soref, G. Sun, and H. H. Cheng, "Electrically-injected GeSn vertical-cavity surface emitters on silicon-on-insulator platforms," submitted to *ACS Photonics*
5. J. Margetis, Y. Zhou, W. Dou, P. Grant, B. Alharthi, W. Du, A. Wadsworth, Q. Guo, H. Tran, S. Ojo, G. Abernathy, A. Mosleh, S. Amir Ghetmiri, G. Thompson, J. Liu, G. Sun, R. Soref, J. Tolle, B. Li, M. Mortazavi, and S.-Q. Yu, "All group-IV SiGeSn/GeSn/SiGeSn QW laser on Si operating up to 90 K," *Applied Physics Letters* **113**, 221104 (2018)
6. W. Dou, Y. Zhou, J. Margetis, S. A. Ghetmiri, S. Al-Kabi, W. Du, J. Liu, G. Sun, R. A. Soref, J. Tolle, B. Li, M. Mortazavi, and S.-Q. Yu, "Optically pumped lasing at 3 μm from compositionally graded GeSn with Sn up to 22.3%," *Optics Letters* **43**, 4558-4561 (2018)
7. J. Margetis, S. Al-Kabi, W. Du, W. Dou, Y. Zhou, T. Pham, P. Grant, S. Ghetmiri, A. Mosleh, B. Li, J. Liu, G. Sun, R. Soref, J. Tolle, M. Mortazavi, S.-Q. Yu, "Si-based GeSn lasers with wavelength coverage of 2–3 μm and operating temperatures up to 180 K," *ACS Photonics* **5**, 827–833 (2018)